

POWER AND SIGNAL MULTIPLEXING FOR ELECTRIC VEHICLES USING CASCADING MULTILEVEL INVERTERS

1. RAVADA ESWAR, 2. KILIMI MANOHAR REDDY, 3. KARANAM LAVANYA,
4. TELU DURAGA PRASAD, 5. *YARRA NAVEEN KUMAR, Assistant Professor.

DEPARTMENT OF ELECTRICAL AND ELETRONICS ENGINEERING

SANKETIKA VIDYA PARISHAD ENGINEERING COLLEGE, VISAKHAPATNAM

ABSTRACT: P&SMT, or power & signal multiplex transmission, is a method for transmitting communication signals using power electronic circuits. A three-phase cascaded multilevel inverter-based P&S MT system is suggested in this paper. By transmitting communication signals without using a Controller Area Network bus, the suggested solution can lower the wiring expense of the existing electric vehicle (EV) communication system. The system's architecture enables battery balancing discharge and motor speed management for EVs. In a simulation model constructed in Matlab/Simulink, both power and communication signals are effectively conveyed using the combined pulse width modulation scheme and frequency shift keying approach. The maximum signal rate of the suggested system is determined to be 600 bit/s by analysing the bit error rate of the sent signal.

Index Terms—Battery state of charge, controller area network, frequency shift keying, motor speed control, pulse width modulation, three-phase DC-AC converter.

LINTRODUCTION

The difficulties posed by climate change are motivating experts and academics to look into fossil fuel substitutes in order to reduce carbon dioxide emissions. These days, the use of electric vehicles offers a workable alternative for energy savings and emission reduction in the automotive industry. Electric vehicles (EVs) create less noise and air pollutants like CO and NO_x than conventional internal combustion engine vehicles (ICEVs) do [1], [2]. Additionally, charging an EV battery at night can help the grid balance the load and save costs by avoiding the peak in power usage [3]. It is vital to use an efficient approach to realise signal transmission since several subsystems, including the motor control unit (MCU) and the battery management system (BMS) in an EV, need communication with the transmission control unit (TCU) [4], [5]. Because of its high reliability and high communication baud rate, using a Controller Area Network (CAN) bus for data transmission in electric vehicles is one of the methods that is widely acknowledged by manufacturers and researchers [6], [7]. Fig. 1 shows the general layout of an EV's powertrain. For a 2-level inverter, several traditional power systems for EVs use a DC/DC converter to increase the battery voltage [8], [9]. This method may result in large switching losses due to its rapid voltage change rates (dV/dt) [8]. Due to the usage of large inductors for the DC/DC boost converters, the system is both expensive and has low power density [9]. Traditional EVs use the CAN bus to realise their internal communication, but the power transmission line and the communication channel are still two separate parts of the system that can still be optimised. In

order to transmit power and communication signals simultaneously through a three-phase multilevel inverter circuit for EVs, the power and signal multiplex transmission (P&SMT) approach is proposed in this study. A DC/DC converter is not necessary since the cascaded multilevel inverter itself may increase the battery voltage because the individual devices of the multilevel inverter have substantially lower switching losses than those of a 2-level inverter. Further paper is extended using three Level Converter. And switching can be reduced more. In the suggested system, frequency shift keying (FSK) is used to modulate the transmitted signals while pulse width modulation (PWM) is used to convert power. The proposed method can significantly reduce the cost of the communication system because the power and signals are delivered simultaneously using the same power line, as opposed to using a CAN bus as a communication channel in modern EVs. The rest of this essay is organised as follows. The suggested system's structure and P&SMT methods are described in Section II. Multi-Level Converters are Explained in section III. Section IV presents the simulation findings. A brief conclusion is drawn in Section V at the end of this study.

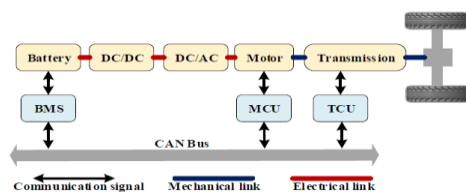


Fig 1: Schematic Diagram of EV integration

II. PROPOSED P&SM TRANSMISSION SYSTEM

I. System Structure:

In this study, the transmitted battery state of charge (SOC) signal and the motor speed control signal are used as examples to further explain the fundamentals of the proposed P&SMT approach. Fig. 2 depicts the suggested system architecture for an EV employing the P&SMT approach. Signals are transmitted through a three-phase multilevel inverter circuit to enable communication between the battery and BMS as well as between the MCU and motor. Fig. 3 shows the suggested structure of a three-phase P&SMT system. Each phase of the inverter architecture consists of four series-connected H-

bridge cells, one of which is driven by a DC voltage source and is used for signal transmission, while the remaining three cells are battery-powered and are used for energy transmission. The phase A and phase B branches, respectively, are used to carry the SOC signal and the motor speed adjustment signal. In this example, the inverter topology's load is a permanent magnet synchronous motor (PMSM).

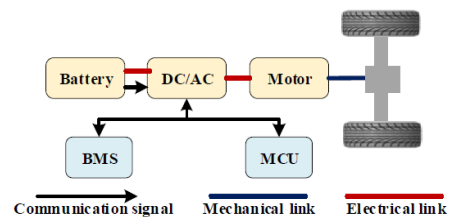


Figure 2: System architecture for an EV employing the P&SMT approach

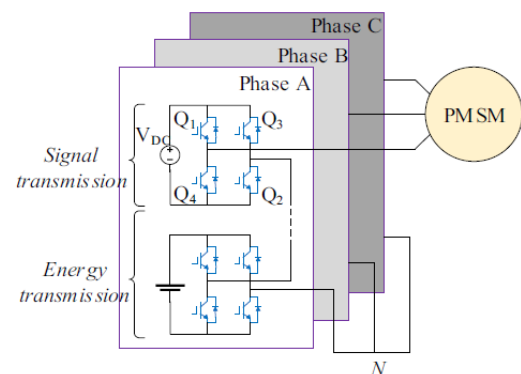


Figure 3. Topology of the proposed P&SMT system for EVs.

B. Signal Transmission

In the suggested system, the signals are modulated utilising the FSK method, and the signal transmission scheme can be seen in Fig. 4. Two carriers with different frequencies, as illustrated in SC, can be used to modulate the digital bits '1' and '0', respectively, if the transmitted 4-bit signal SI is '1010'. The signal can be modified by managing the quick flipping of the four switches in the cell because it is intended to be relayed through an H-bridge cell in each phase. A switch will specifically turn on if a gate signal of digital '1' is applied and turn off if a gate signal of digital '0' is applied. The switches Q3 and Q4 turn on and off

simultaneously in Fig. 3, and Q1 and Q2 function concurrently. Additionally, so as to prevent a short circuit, switches Q1 and Q2 work in the opposite state from switches Q3 and Q4. The transmitted signal can be thought of as overlaid on the output current waveform since the H-bridge cell used for signal transmission is series linked with the other three cells used for energy transmission. The transmitted signal is then extracted from the output current waveform at the receiver using a band-pass filter. The Fourier series expansion of any signal $f(x)$ with period T and angular frequency $=2\pi/T$ can be written as

$$F(x) = \frac{1}{2}a_0 + \sum_{n=1}^{\infty}(a_n \cos n\omega x + b_n \sin n\omega x) \tag{1}$$

Where a_0 , a_n , b_n defined as:

$$\left\{ \begin{aligned} a_0 &= \frac{2}{T} \int_{-T/2}^{T/2} f(x) dx \\ a_n &= \frac{2}{T} \int_{-T/2}^{T/2} f(x) \cos n\omega x dx \\ b_n &= \frac{2}{T} \int_{-T/2}^{T/2} f(x) \sin n\omega x dx \end{aligned} \right. \tag{2}$$

Similarly, if a square wave $f(t)$ with period T is applied as a carrier for digital '1', it can be expressed as

$$f(t) = \begin{cases} 0 & -\frac{T}{2} \leq t < 0 \\ 1 & 0 \leq t \leq \frac{T}{2} \end{cases} \tag{3}$$

The Fourier series expansion of $f(t)$ is derived as

$$F(t) = \frac{1}{2} + \frac{2}{\pi} \sin x + \frac{2}{3\pi} \sin 3x + \frac{2}{5\pi} \sin 5x + \frac{2}{7\pi} \sin 7x + \dots + \frac{2}{n\pi} \sin nx \tag{4}$$

the number n being odd. The first-order harmonic can be used for restoring the communication signals because the Fourier series expansion of $f(t)$ only contains the odd harmonic components and the first-order harmonic has the biggest amplitude. For instance, the upper envelope of the demodulated carrier for the digital "1" represented by the

curve SD in Fig. 4 can be collected using an envelope detector. When the upper envelope's amplitude exceeds the comparison value and a suitable comparison value is used, the upper envelope can be recovered to a digital '1'. Otherwise, a digital '0' will be recovered. After sampling the recovered digital signal at the SI's initial bit rate, the restored SR is finally acquired.

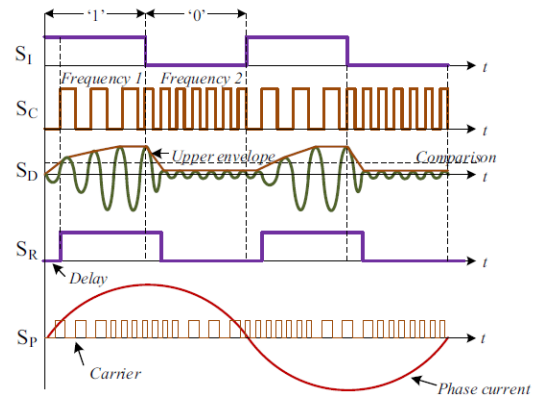


Figure 4: The proposed system's proposed signal transmission scheme,

where SI is the initial 4-bit signal '1010', SC is the carrier waveform, SD is the extracted carrier for the digital '1' after applying a band-pass filter, SR is the restored signal, and SP is the output phase current waveform superimposed with the carrier of the signal.

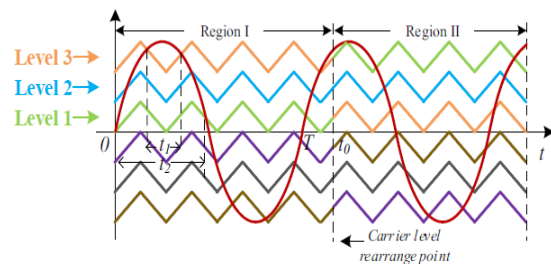


Fig. 5. Carrier level rearrangement in the PWM process.

An envelope detector can be used to obtain the upper envelope of the digital "1" demodulated carrier. When the upper envelope's amplitude exceeds the comparison value and a suitable comparison value is used, the upper envelope can be recovered to a digital '1'. Otherwise, a digital '0' will be recovered. After sampling the recovered digital signal at the SI's initial bit rate, the restored SR is finally acquired.

C. Motor Speed Regulation and Battery Balance Discharging

In the suggested system, the power frequency is varied along with the communicated signal to control the motor speed. The link between a PMSM's motor speed n , pole-pair p , and power frequency f is explicitly shown as

$$n = \frac{60f}{p} \quad (3)$$

where 60 s/min is indicated by the constant 60. A 2-pole pair motor's speed should theoretically fluctuate between 1200 and 1800 r/min if the power frequency ranges between 40 and 60 Hz. The power frequency is then determined using the sent signal s by

$$f = 20 \times s + 40 \quad (4)$$

If the transmitted signal contains a digital '0' or '1', the power frequency will be 40 Hz or 60 Hz, accordingly. The next step is to collect the three-phase reference sinusoidal waves from

$$\begin{cases} P_a = A \sin(2\pi f) \\ P_b = A \sin\left(2\pi f - \frac{2}{3}\pi\right) \\ P_c = A \sin\left(2\pi f - \frac{4}{3}\pi\right) \end{cases} \quad (5)$$

where A is the amplitude and P_a , P_b , and P_c , respectively, stand in for the reference wave in phases A, B, and C. The phase A reference wave is $2/3$ and $4/3$ radians behind the phase B and phase C reference waves, respectively. Finally, the motor is driven by modulated variable frequency sine waves in order to alter the motor speed.

The gating signal of a switch is created using the traditional sinusoidal PWM method by comparing the reference wave with a triangular carrier. The duty cycle of each switch varies

because different carriers and the reference wave meet at distinct locations.

As shown in Fig. 5, for instance, in a single period from 0 to T , a switch controlled by a "Level 3" carrier has a lower duty cycle than a switch modulated by a "Level 1" carrier ($t1t2$). The switch operating with a reduced duty cycle uses less power than the switch operating with a bigger duty cycle since the input power is provided by batteries. This will also increase the likelihood that, after the system has been functioning for some time, the batteries' remaining capacity will be out of balance. Therefore, by periodically rearranging the carrier levels inside the PWM process, the battery balance discharging can be achieved.

To accomplish this goal, a data stream created from the battery SOC values at the periodic sampling point is first communicated via the FSK method through a full-bridge cell powered by a DC voltage source. The SOC values are divided into various decimal numbers once the signal from the phase current has been demodulated. Finally, the battery balance discharge is accomplished by rearranging the PWM carrier levels in accordance with the communicated SOC values (at t_0 in Fig. 5, for example).

Parameter name	Value
DC voltage source	30 V
Battery voltage	48 V
PWM carrier frequency	2 kHz
PWM referenced sine wave frequency	40 Hz, 60 Hz
Carrier frequency of motor speed adjustment signal	4 kHz for '1' and 8 kHz for '0'
Carrier frequency of SOC signal	6 kHz for '1' and 10 kHz for '0'

TABLE I
PARAMETERS VALUE USED IN THE PROPOSED SYSTEM
III MATLAB/SIMULINK IMPLEMENTATION

A. Simulation Parameters and Output Waveforms

Matlab/Simulink is used to create a simulation model as shown in figure 6 The parameter values for the simulation model are summarised in Table I. A 48 V battery is installed in each H-bridge cell for power transmission, and a 30 V DC voltage source is used in each H-bridge circuit for signal transmission. As a result, neither the transmitted signal's amplitude is too tiny to allow for restoration nor is it too great to significantly alter the output sinusoidal waveform. Additionally, silicon type IGBT devices can work in this frequency range because the system uses carriers with a frequency distribution of 2 kHz to 10 kHz

Fig. 7 shows the output voltage and current waveforms measured by a voltage sensor and a current sensor when a PMSM is connected to the output side of a three-phase inverter circuit as a load. The maximum phase voltage is 174 V ($348+30=174$) due to the three batteries and a DC voltage source in each phase. It is noticeable that the phase current waveform's amplitude differs at approximately 0.27 s and 0.51 s. This is due to the motor power frequency switching from 40 Hz to 60 Hz at these time intervals.

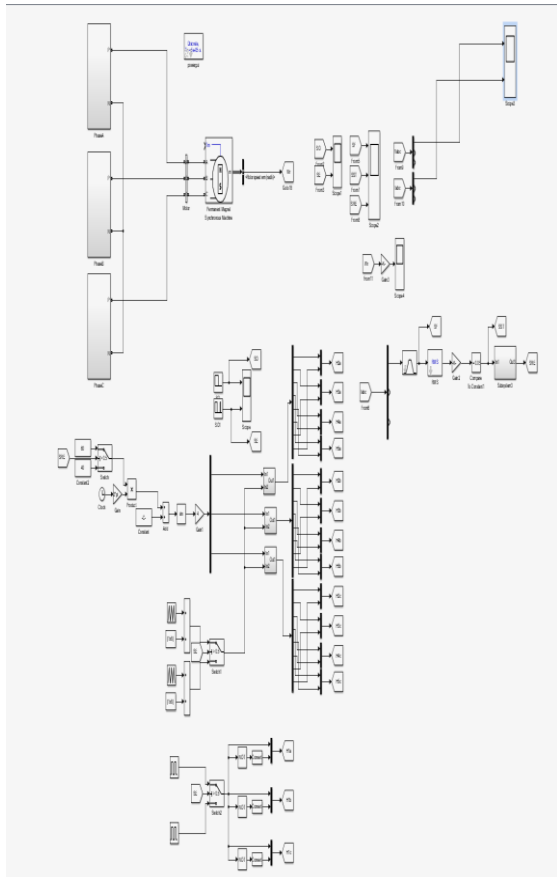


Fig6: MATLAB Implementation

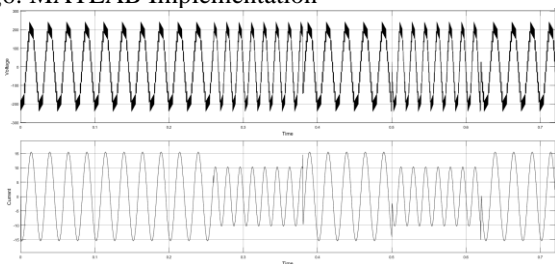


Fig 7: Output Voltages and Currents

B. B. Motor Speed Adjustment Signal Transmission:

Since an original 8-bit motor speed adjustment signal has a bit length of 0.03 s, its transmitting rate is 100/3 bps. Then, to distinguish between two adjacent 8-bit data strings, a 4-bit cyclic redundancy code (CRC) is inserted at the end of each data string. The complete 12-bit data frame is 111100000100 since the created 4-bit CRC code is 0100 thanks to the generator $x^4 + x^3 + x^2 + x + 1$. By using the modulo-2 division method and the divisor 11110 to

divide the transmitted data frame, the system can check to see if the residual is zero to see if the frame data is incorrect. By using the modulo-2 division method and the divisor 11110 to divide the transmitted data frame, the system can check to see if the residual is zero to see if the frame data is incorrect. If it is 0, it demonstrates that there were no transmission faults in the frame data; if not, there was a problem. Figure 8 displays both the initial message data and the message data after the CRC code.

It is important to note that the time required to send a frame with and without a CRC code is the same; as a result, the 12-bit data is transmitted at a rate of 0.02 s per bit. The 4 kHz square wave is utilised as a carrier for digital "1" and the 8 kHz square wave is used as a carrier for digital "0" after the whole data frame has been collected.

The 4 kHz carrier is then recovered from the phase current waveform with a band-pass filter after the signal has passed through an H-bridge cell. The transmitted signal is then recovered with the help of the suitable threshold value using the filtered carrier waveform SF in Fig. 9.

Since this band-pass filter's attenuation at cut-off frequencies is fixed at 6 dB, the attenuation ratio x can be derived as 0.5 from

$$20 \log x = -6 \quad (6)$$

Finally, Fig. 9's recovered signal SRE is used to

control the motor speed, which is shown in Fig. 10's waveform. The motor turns on whenever the signal shifts from '0' to '1'. Speed varies for roughly 0.01 seconds. The motor speed stabilises between 1200 r/min and 1800 r/min as expected because the power frequency is made to alternate between 40 Hz and 60 Hz. The sent signal will interfere with the phase current waveform because it is superposed on the phase current as energy, which will impact the stability of the motor speed. The steady-state variation of the motor speed, which is open-loop controlled by varying the motor power frequency, is also greater than that of the traditional double closed-loop control strategy.

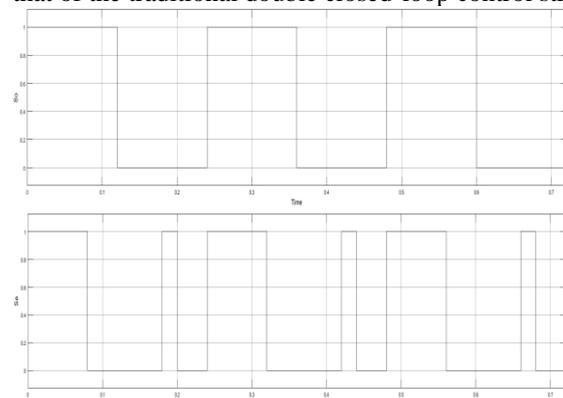


Fig. 8. So represents for the original 8-bit data string and Ss refers to the entire 12-bit transmitted signal.

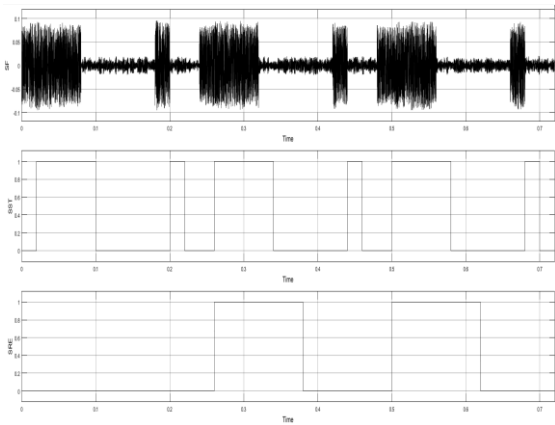


Fig 9 SF represents the extracted 4 kHz carrier after the filtering process; SST is the recovered 12-bit signal; SRE is the restored 8-bit motor speed adjustment signal.

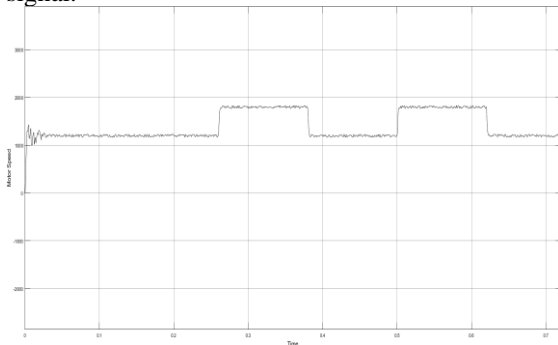


Fig. 10. The controlled motor speed with the transmitted 8-bit signal '11110000'.

Conclusion:

In this research, a three-phase multilevel inverter-based P&SMT system is suggested to enable battery balance discharging and motor speed adjustment for EVs. Each phase of the inverter architecture involves four series-connected H-bridge cells, three of which are controlled by PWM for energy transmission and the remaining two by FSK for signal transmission. The complexity of the overall system can be decreased by simplifying the system wiring since the suggested technique uses a portion of the power electronic circuit as a communication channel. The viability of the proposed P&SMT technique is tested by sending the battery SOC signal and the motor speed adjustment signal through the phase-A and phase-B currents, respectively, using a simulation model that has been constructed in matlab/Simulink. Additionally, after examining the connection between the signal bit rate and error rate, it is established that the suggested method's signal transmission capability is 600 bit/s.

REFERENCES

- [1] T. Donato, F. Licci, A. D'Elia, G. Colangelo, D. Laforgia and F. Ciancarelli, "Evaluation of emissions of CO₂ and air pollutants from electric vehicles in Italian cities," *Applied Energy*, vol. 157, pp. 675-687, Nov. 2015.
- [2] C. Ma, C. Chen, Q. Liu, H. Gao, Q. Li, H. Gao and Y. Shen, "Sound quality evaluation of the interior noise of pure electric vehicle based on neural network model," *IEEE Transactions on Industrial Electronics*, vol. 64, no. 12, pp. 9442-9450, 2017.
- [3] M. Yilmaz and P. T. Krein, "Review of the impact of vehicle-to-grid technologies on distribution systems and utility interfaces," *IEEE Transactions on Power Electronics*, vol. 28, no. 12, pp. 5673-5689, 2013.
- [4] K.Ç. Bayindir, M.A. Gözüktüçük and A. Teke, "A comprehensive overview of hybrid electric vehicle: Powertrain configurations, powertrain control techniques and electronic control units," *Energy Conversion and Management*, vol. 52, no. 2, pp. 1305-1313, 2011.
- [5] X. Zhu, H. Zhang, J. Xi, J. Wang and Z. Fang, "Optimal speed synchronization control for clutchless AMT systems in electric vehicles with preview actions," *2014 American Control Conference*, pp. 4611-4616, 2014.
- [6] F. Zhou, S. Li and X. Hou, "Development method of simulation and test system for vehicle body CAN bus based on CANoe," *2008 7th World Congress on Intelligent Control and Automation*, pp. 7515-7519, 2008.
- [7] M. Zheng, B. Qi and H. Wu, "A li-ion battery management system based on CAN-bus for electric vehicle," *2008 3rd IEEE Conference on Industrial Electronics and Applications*, pp. 1180-1184, 2008.
- [8] L. M. Tolbert, F. Z. Peng and T. G. Habetler, "Multilevel inverters for electric vehicle applications," *Power*

Electronics in Transportation (Cat. No.98TH8349),
pp. 79–84, 1998.

[9] Z. Du, B. Ozpineci, L. M. Tolbert and J. N. Chiasson, "DC-AC cascaded H-bridge multilevel boost inverter with no inductors for Electric/Hybrid electric vehicle applications," *IEEE Transactions on Industry Applications*, vol. 45, no. 3, pp. 963–970, 2009.

[10] L. Lampe, A.M. Tonello and T.G. Swart, *Power Line Communications: Principles, Standards and Applications from multimedia to smart grid*, John Wiley & Sons, 2016.